Publication Date: 02 September 2026
Archs Sci. (2026) Volume 75, Issue 6 Pages 31-39, Paper ID 2025604.
https://doi.org/10.68304/as/75604

Hydrogen Demand and Carbon Retention in Methanol Production From Plastic-Derived Syngas

Georgi E. Karadzhov and Maria Ivanova
Institute of Mathematics and Informatics, Bulgarian Academy of Sciences, 1113 Sofia, Bulgaria
Corresponding authors: Georgi E. Karadzhov (e-mail: georgikaradzhov@gmail.com).

Abstract A high H_2/CO ratio can overstate the suitability of plastic-derived synthesis gas for methanol production when CO_2 is also present. This study quantifies the hydrogen requirement and carbon-retention limit of ten-batch polyethylene-reforming gas containing 229.3 mmol H_2, 95.1 mmol CO, 37.7 mmol CO_2, and 36.9 mmol CH_4. An analytical stoichiometric bound is verified by reaction-network linear programming and used to compare hydrogen addition, selective CO_2 removal, water–gas shift, and conditional methane reforming. Despite an H_2/CO ratio of 2.411, the gas has a methanol stoichiometric number of 1.443 and a 74.0 mmol hydrogen deficit. Without additional hydrogen, the methanol ceiling is 108.13 mmol, corresponding to 81.43% of the initial carbon-oxide carbon. Removing 24.67 mmol CO_2 balances the retained gas without increasing this ceiling; adding 74.0 mmol H_2 instead permits retention of all 132.8 mmol carbon oxides. Water–gas shift leaves the deficit unchanged. Complete steam reforming of the measured methane would raise the ceiling to 157.33 mmol but leave a 37.1 mmol hydrogen deficit for the enlarged carbon pool. Independent $\pm 5\%$ composition perturbations give deficits of 47.37–100.63 mmol. Numerical and analytical results agree across 10,201 conditioning points. The results quantify the carbon cost of reducing external hydrogen demand; they are stoichiometric limits, not measured methanol yields or predictions of plant performance.

Index Terms polyethylene reforming, methanol, hydrogen sufficiency, carbon dioxide removal, reaction-network optimization, deterministic sensitivity

I. Introduction

Converting waste plastic into synthesis gas does not, by itself, establish how much of its carbon can be recovered in a chemical product. For methanol, that question depends on the balance among hydrogen, carbon monoxide, and carbon dioxide. A gas with an H_2/CO ratio above two may still contain too little hydrogen to convert all its carbon oxides. Selective CO_2 removal can correct the composition, but does so by reducing the carbon available for synthesis. Assessing a plastic-to-methanol route therefore requires a product-specific balance alongside the upstream gas yield.

This distinction is relevant to the broader aims of plastics recycling. Historical material-flow analysis documents the accumulation of plastic waste [1], while carbon-footprint studies show that energy supply, recycling, and material demand affect different parts of its environmental burden [2]. Circular-carbon strategies combine material recovery with low-carbon energy [3]; assessments against planetary boundaries further show that climate performance is only one sustainability criterion [4]. Comparisons of recycling technologies consequently consider product quality and subsequent processing, as well as conversion [5], [6]. In methanol production, the carbon lost during gas conditioning belongs in that comparison.

Plastic-derived synthesis gas has been produced using nickel-impregnated zeolites [7], controlled steam addition in pyrolysis–gasification systems [8], iron–nickel catalysts supported on MCM-41 [9], and sacrificial tire-char catalysts [10]. These routes produce different proportions of carbon oxides, hydrogen, and residual hydrocarbons. Electrification adds another process variable: Joule-heated dry reforming has been demonstrated for plastics [11], and electrically heated methane reformers place the heat source within the reacting structure [12]. Neither the heating method nor the total hydrogen yield specifies whether the resulting gas meets the requirements of methanol synthesis.

Process studies have examined electrified methane reforming for methanol production [13], pilot-scale electrified biogas reforming [14], and the transient response of electrically heated reformers [15]. Their results depend on feed composition, heat transfer, and operating conditions. A gas balance offers a more limited, but useful, preliminary test: it determines whether the available reactants could supply a target product before reactor performance is considered. Hydrogen yield normalized to polymer hydrogen is unsuitable for this purpose because water can also supply hydrogen during reforming. The relevant comparison is between the measured hydrogen

amount and the demand associated with all carbon intended for synthesis.

Methanol-feed adjustment by separation is well established. Ribeiro and colleagues examined pressure-swing adsorption for stoichiometric adjustment and CO_2 capture [16]. The resulting feed still has to be evaluated against catalytic requirements. Studies of Cu/ZnO active sites [17], indium-oxide microkinetics [18], and industrial copper-based catalysts [19] describe behavior that an elemental balance cannot predict. A stoichiometrically sufficient mixture may have an unfavorable rate, equilibrium conversion, or water content; conversely, a hydrogen-deficient mixture can produce some methanol while leaving carbon unconverted.

The same separation of questions is needed at plant level. Water management and heat integration affect methanol-process performance [20], while techno-economic assessments require an explicit hydrogen source and utility inventory [21]. Biomass- and CO_2-derived methanol have different process constraints despite yielding the same molecule [22]. Variable electricity introduces a further choice between flexible operation and storage [23], [24]. An aggregate gas composition cannot resolve these design questions, but it can establish the material requirement that a later process model must satisfy.

Here, a ten-batch polyethylene-reforming record is used to quantify that requirement. The analysis asks how much carbon-oxide carbon can enter methanol, how hydrogen addition and selective CO_2 removal change the limit, and whether water–gas shift or conversion of the measured methane can close the hydrogen balance. A reaction-network linear program is compared with a closed-form bound, then evaluated under prescribed composition perturbations. The contribution is a composition-specific assessment of conditioning choices; the stoichiometric number, shift chemistry, and optimization method are established tools. All principal comparisons use the same aggregate gas vector, avoiding combinations of measurements from different experimental scales or operating conditions.

II. Materials and methodology

A. Gas record, attribution, and inclusion rules

The empirical basis is the ten-batch polyethylene-reforming experiment [25]. Table 1 distinguishes experimental quantities from calculation constants. All amounts refer to the aggregate campaign; the ten batches are not treated as independent composition replicates. The principal carbon denominator is the sum of CO and CO_2, whose molecular identities and amounts are specified. Methane is included only in the separate reforming calculation. The C_{2+} group has no assigned average formula, and solid carbon is excluded from the methanol balance.

Table 1: Experimental inputs and fixed calculation constants

Quantity	Value	Unit
H_2	229.3	mmol
CO	95.1	mmol
CO_2	37.7	mmol
CH_4	36.9	mmol
Polyethylene	2.5	g
Water	5.5	g
Electricity	2939.76	kJ
Polyethylene energy	114.75	kJ
H_2 higher heating value	286	kJ mol^{-1}
CO higher heating value	283	kJ mol^{-1}
Methanol formula mass	32.04	g mol^{-1}
H_2 formula mass	2.016	g mol^{-1}

The aggregate record does not provide a covariance matrix or replicate distribution for these gas amounts. In addition, the three CO entries printed in Supplementary Table 3 do not reproduce the mean and standard deviation printed there. They are therefore not used to estimate measurement uncertainty. The grouped-hydrocarbon information likewise does not establish a unique molecular composition. Input values, source locations, and exclusions are recorded in the accompanying machine-readable input file.

B. Reaction-network allocation and analytical ceiling

Let h, c, and d denote the initial amounts of H_2, CO, and CO_2, respectively. Let a be added hydrogen and r selectively removed carbon dioxide, with $0 \le r \le d$. The idealized reaction set consists of CO hydrogenation, CO_2 hydrogenation, and signed water–gas shift. Water may enter or leave as required; its preparation and removal duties are outside this molecular allocation. Methane and heavier hydrocarbons are nonreacting components unless the separate methane conversion is activated.

$$\left.\begin{aligned} \mathrm{CO} + 2\mathrm{H_2} &\longrightarrow \mathrm{CH_3OH}, \\ \mathrm{CO_2} + 3\mathrm{H_2} &\longrightarrow \mathrm{CH_3OH} + \mathrm{H_2O}, \\ \mathrm{CO} + \mathrm{H_2O} &\rightleftharpoons \mathrm{CO_2} + \mathrm{H_2}. \end{aligned}\right\} \tag{1}$$

The different hydrogen coefficients make carbon dioxide relevant even when the hydrogen-to-carbon-monoxide ratio exceeds two. Define the carbon-oxide amount C, methanol stoichiometric number S, and full-carbon hydrogen deficit D by

$$C = c+d, \qquad S = \frac{h-d}{c+d}, \qquad D = 2c+3d-h = C(2-S). \tag{2}$$

A positive deficit indicates insufficient hydrogen for complete conversion of both carbon oxides within the specified reaction set. It is not a statement about the amount that will react during a finite residence time. The stoichiometric number is defined only when carbon oxides are present; the implementation handles empty feeds separately without dividing by zero.

Let x and y be methanol formed through the first two reactions, and let z be the signed forward-shift extent. The op-

ARCHIVES DES SCIENCES
A Multidisciplinary Journal

timization maximizes methanol while requiring nonnegative residual gas amounts:

$$\begin{cases} M_{\max} = \max\limits_{x,y,z} x + y, \\ \qquad x + z \le c, \\ \qquad y - z \le d - r, \\ 2x + 3y - z \le h + a, \\ \qquad x, y \ge 0, \qquad -(d - r) \le z \le c. \end{cases} \tag{3}$$

Water is available without a supply constraint, but the network contains no independent water-splitting reaction. Forward shift can generate hydrogen only by converting CO into CO_2. Thus, a hydrogen-free CO feed can allocate some carbon to methanol by releasing the rest as CO_2; it cannot convert all its carbon. Eq. (3) enforces the material balances while relaxing equilibrium, kinetic, and heat-transfer constraints.

The signed extent avoids restricting the calculation to an arbitrarily chosen reaction sequence. Summing the carbon inequalities gives $x + y \le c + d - r$. Summing the CO and hydrogen inequalities gives $3(x + y) \le h + c + a$. Consequently,

$$M_{\max} = \min\left(c + d - r, \frac{h + c + a}{3}\right). \tag{4}$$

The equality is attainable in this stoichiometric relaxation. When hydrogen is sufficient, $x = c$, $y = d - r$, and $z = 0$ consume all retained carbon oxides. In the hydrogen-limited region with $h + a \ge 2c$, choosing $x = c$, $y = (h + a - 2c)/3$, and $z = 0$ attains the second bound. When $h + a < 2c$, choosing $y = 0$, $x = (h + a + c)/3$, and $z = c - x$ attains it by sacrificing part of the CO through forward shift. These constructions prove the bound without assuming a catalyst can independently select the indicated extents.

C. Conditioning choices and composition targets

Complete conversion of retained carbon oxides requires enough hydrogen after removal. For a retained-gas stoichiometric number of at least two, the minimum addition is

$$a_{\min}(r) = \max(0, D - 3r). \tag{5}$$

Each removed millimole of carbon dioxide reduces the complete-conversion hydrogen requirement by three millimoles, but also removes one millimole of potential methanol carbon. This exchange rate is a chemical relation, not a cost ratio. The analysis also evaluates specified feed targets $s = 2.05$ and 2.10 to show the effect of an intentional hydrogen excess:

$$a_{\min}(r; s) = \max\{0, D + (s - 2)C - (s + 1)r\}. \tag{6}$$

Eq. (6) specifies $S \ge s$: where the expression inside the maximum is positive, addition reaches $S = s$; where it is negative, removal alone has already exceeded the target. The values 2.05 and 2.10 are illustrative margins, not universal catalyst requirements. Carbon retention is reported as $M_{\max}/C$ relative to the initial CO and CO_2 amount. If all retained carbon oxides are converted after removal, this fraction is $(C - r)/C$.

D. Shift invariance and conditional methane conversion

For a forward-shift extent z, the gas becomes $(h+z, c-z, d+z)$. Direct substitution gives

$$D(z) = D, \qquad S(z) = S, \qquad h(z) + c(z) = h + c. \tag{7}$$

Thus, shift alone leaves the full-carbon deficit and the allocation ceiling unchanged even though it changes the H_2/CO ratio. This invariance applies to the stated closed carbon-oxide balance; removal of carbon dioxide after shift is a different operation. The numerical comparison varies forward shift from zero to 60 mmol, remaining below the available CO amount and avoiding a divergent ratio.

For methane, ideal steam reforming is applied to a selected extent t between zero and the quantified 36.9 mmol. The reaction and its consequences are

$$\begin{cases} \mathrm{CH_4 + H_2O \longrightarrow CO + 3H_2}, \\ \quad (h_t, c_t, d_t) = (h + 3t, c + t, d), \\ \qquad D_t = D - t, \qquad C_t = C + t. \end{cases} \tag{8}$$

Methane conversion is a conditional downstream choice, not an additional observed conversion. Its thermal feasibility, catalyst requirement, and water duty are not supplied by this equation. Numerical investigation of electrically heated structured reformers illustrates why those questions require a separate transport and reaction model [26].

E. Deterministic tolerances and computational verification

Independent multiplicative perturbations of h, c, and d are prescribed with relative half-widths $\varepsilon = 0.01$, 0.05, and 0.10. All eight corners of each box are evaluated. Since the deficit is affine in the quantities, its exact extreme values over each box are

$$D_{\min,\max} = D \mp \varepsilon(2c + 3d + h). \tag{9}$$

The boxes test sensitivity to specified discrepancies; they are not confidence regions, distributions of plastic waste, or empirical estimates of analytical precision. Unlike statistically constructed uncertainty sets [27], their widths are chosen explicitly for deterministic inspection. Independent perturbations need not preserve the upstream elemental balance, which is appropriate for a measurement-consistency stress test but not for representing additional physically measured feeds.

Array calculations use NumPy [28]; independent linear programs use SciPy [29] with the HiGHS dual-simplex solver [30]. The principal grid contains 101 equally spaced hydrogen additions from zero to 130 mmol and 101 removals from zero to 37.7 mmol. Additional checks include 24 composition corners, 201 methane extents, 201 shift extents, and eight boundary feeds. The analytical and numerical objectives must agree within 10^{-7} mmol. All plots are generated directly from the calculated arrays using Matplotlib [31].

ARCHIVES DES SCIENCES
A Multidisciplinary Journal

F. Electricity boundary

The campaign electricity is divided by the ideal methanol mass to obtain an electricity-only lower bound per unit of attainable product:

$$e_{\mathrm{el,min}} = \frac{E_{\mathrm{el}}}{M_{\max} W_{\mathrm{MeOH}}}, \tag{10}$$

with consistent conversion from millimoles to moles and grams to kilograms. Because actual methanol output cannot exceed the stoichiometric ceiling within this reaction set, the ratio is a lower bound conditional on the recorded electricity, not an estimate of industrial energy consumption. Hydrogen production, synthesis compression, methane reforming, separation, and heat recovery are unquantified. No electricity is deleted from the physical accounting merely because its supply might be photovoltaic.

III. Results and discussion

A. Hydrogen requirement of the reported gas

The initial CO and CO_2 contain 132.8 mmol carbon and require 303.3 mmol H_2 for complete conversion to methanol. The measured 229.3 mmol H_2 leaves a deficit of 74.0 mmol. Although H_2/CO is 2.411, the stoichiometric number is 1.443 because it also accounts for CO_2. The two ratios describe different balances: the first compares hydrogen only with CO, whereas the second measures its sufficiency for the entire carbon-oxide pool. Diluting the gas with an inert carrier would change neither ratio.

The methanol ceiling without conditioning is 108.13 mmol, or 3.465 g, equivalent to 81.43% of the initial carbon-oxide carbon. A feasible zero-shift allocation uses all 95.1 mmol CO and 13.03 mmol CO_2, leaving 24.67 mmol CO_2. This allocation proves that the bound can be reached within the reaction model; it does not imply preferential CO conversion on a real catalyst.

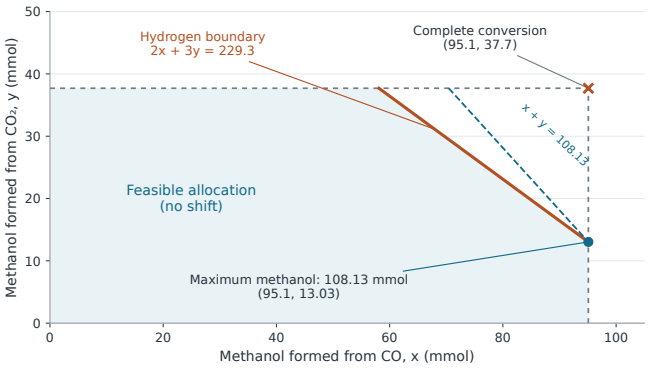

Figure 1: Feasible methanol allocation without added hydrogen or CO_2 removal. Shading satisfies $x \le 95.1$, $y \le 37.7$, and $2x + 3y \le 229.3$ mmol at zero shift. The optimum is $(x, y) = (95.1, 13.03)$ mmol, giving $M_{\max} = 108.13$ mmol. Complete conversion of both carbon oxides lies outside the hydrogen-feasible region. The dashed objective line has $x + y = M_{\max}$

Figure 1 shows why carbon availability alone overestimates the attainable product. The point representing complete conversion of both carbon oxides lies outside the hydrogen-feasible region. Maximizing the sum of the two methanol-forming extents reaches the CO-availability boundary at 108.13 mmol total methanol. Signed shift permits other allocations with the same objective, but cannot raise that objective. Individual solver-selected reaction extents should therefore not be interpreted as identified surface pathways.

The 81.43% value is a carbon-oxide retention fraction, not a recovery percentage for the polyethylene feed. Methane, grouped hydrocarbons, and solid carbon are outside its denominator. As a diagnostic, interpreting each unit of the reported C_{2+} group as a molecule with two carbon atoms gives an apparent total carbon closure of 104.72% on a CH_2 repeat-unit basis. That conditional calculation is insufficient to identify the origin of the discrepancy, but shows why a precise feed-carbon recovery should not be inferred from the aggregate labels. The CO-plus-CO_2 denominator avoids an unsupported assignment to the unresolved group.

B. Trading hydrogen addition against carbon rejection

Adding 74.0 mmol H_2 (0.1492 g) supplies the full nominal deficit and raises the methanol ceiling to 132.8 mmol (4.255 g). With no external hydrogen, removing 24.67 mmol CO_2 instead brings the retained stream to $S = 2$. The removed amount is 65.43% of the initial CO_2 and 18.57% of the initial carbon-oxide carbon. These percentages refer to different inventories and are not interchangeable.

Table 2 includes an intermediate choice: 37.0 mmol added hydrogen and 12.33 mmol removed CO_2 give a 120.47 mmol ceiling and retain 90.71% of the initial carbon oxides. Selective removal alone has the same 108.13 mmol ceiling as the untreated gas because it removes carbon that the available hydrogen cannot support. Hydrogen addition increases product potential by supplying reducing equivalents without discarding carbon.

Table 2: Nominal conditioning choices and their stoichiometric methanol ceilings. Carbon retained is $100M_{\max}/132.8$, using the initial CO-plus-CO_2 carbon inventory. Selective removal assumes no loss of H_2 or CO

Condition	Added H_2 mmol	Removed CO_2 mmol	Methanol ceiling mmol	Carbon retained %
Unconditioned gas	0	0	108.13	81.43
Selective removal	0	24.67	108.13	81.43
Mixed adjustment	37.0	12.33	120.47	90.71
Hydrogen addition	74.0	0	132.80	100.00

The $S = 2$ boundary in Figure 2 has a slope of -3: each millimole of CO_2 removed reduces hydrogen demand by 3 mmol. Points above the boundary have sufficient hydrogen for all retained carbon oxides; points below it remain deficient. Along the boundary, both composition and potential carbon retention change. Its endpoints are therefore alternatives with different material consequences, not equivalent ways of obtaining the same methanol amount.

ARCHIVES DES SCIENCES
A Multidisciplinary Journal

An operating margin raises the requirement. To reach $S = 2.10$ without carbon removal requires 87.28 mmol additional H_2, compared with 74.0 mmol at exact stoichiometry. With no addition, the corresponding removal is 28.15 mmol CO_2. Once removal exceeds the zero-addition intercept, the retained gas has a stoichiometric number above the selected target. The horizontal portions of the curves denote zero required addition, not constant composition.

These boundaries assume perfectly selective CO_2 separation. An actual adsorption or absorption unit may lose hydrogen or CO, consume compression work, and deliver a time-varying product. A mixed-gas purge is particularly different because it can discard hydrogen as well as carbon. The calculation also leaves the destination of removed CO_2 unspecified. Venting, subsequent utilization, and storage have different environmental consequences, so a smaller hydrogen requirement cannot be equated with a smaller carbon footprint.

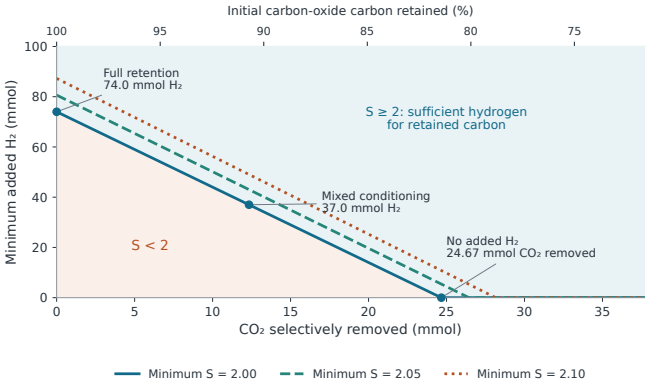

Figure 2: Hydrogen addition required to meet selected minimum stoichiometric numbers after selective CO_2 removal. The solid $S = 2.00$ boundary separates hydrogen-deficient and stoichiometrically sufficient retained feeds. Marked points show full retention, mixed conditioning, and removal without hydrogen addition. The top axis gives retained carbon-oxide carbon relative to the initial 132.8 mmol, assuming complete conversion. Beyond each zero-addition intercept, removal alone exceeds the specified target

C. Where further carbon dioxide removal reduces product potential

At fixed hydrogen addition, Eq. (4) compares a constant hydrogen-limited ceiling with a declining retained-carbon inventory. Removal initially leaves the ceiling unchanged; after the two bounds intersect, each further millimole removed lowers the methanol ceiling by one millimole. Figure 3 locates this transition for three addition levels.

With no added H_2, the transition occurs at 24.67 mmol removal and 108.13 mmol methanol. Adding 37.0 mmol H_2 moves it to 12.33 mmol removal and 120.47 mmol methanol. At 74.0 mmol addition, the untreated gas is already stoichiometrically sufficient, so any subsequent removal reduces the maximum product. All three curves eventually follow the same retained-carbon bound.

A flat part of these curves does not establish that separation is unnecessary. Lower CO_2 content can affect water formation, catalyst behavior, and synthesis-loop operation. Composition-dependent active-site behavior [17] and zinc promotion of copper-based catalysts [32] are relevant to actual productivity. Those effects require a catalytic model or measurements; they do not change the carbon inventory represented by the descending branch. The carbon-maximizing choice and the operating optimum may therefore differ.

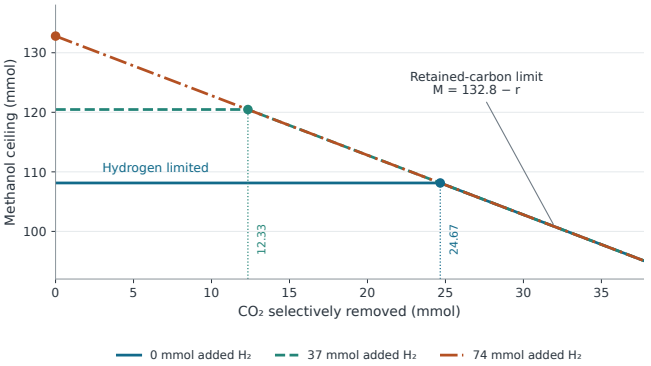

Figure 3: Stoichiometric methanol ceilings at 0, 37, and 74 mmol added H_2. Horizontal segments are hydrogen limited; the common descending segment is limited by retained carbon. Circles mark the transition between bounds. Removal beyond a transition decreases the product ceiling without reducing the selected hydrogen addition

D. Water–gas shift changes the ratio, not the deficit

Shifting 60 mmol CO raises H_2/CO from 2.411 to 8.242, yet leaves $S = 1.443$, $D = 74.0$ mmol, and $M_{\max} = 108.13$ mmol. Each millimole of hydrogen generated is accompanied by conversion of CO to CO_2, increasing the hydrogen needed to retain that carbon by exactly one millimole. Supply and full-carbon demand rise together.

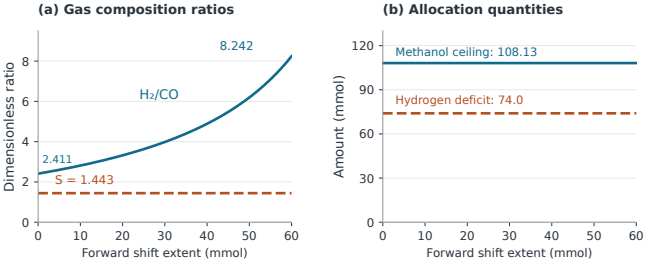

Figure 4: Effect of forward water–gas shift on the nominal gas. (a) H_2/CO rises from 2.411 to 8.242 over 0–60 mmol shift, while the stoichiometric number remains 1.443. (b) The full-carbon hydrogen deficit and methanol ceiling remain 74.0 and 108.13 mmol, respectively. No hydrogen addition or carbon removal is applied

ARCHIVES DES SCIENCES
A Multidisciplinary Journal

The paired panels in Figure 4 distinguish the changing gas ratio from the unchanged allocation limit. A large increase in H_2/CO therefore gives no evidence that shift alone has corrected this gas for full-carbon methanol synthesis. The invariance follows from the balances and holds throughout the physically admissible signed-shift range, not only over the plotted interval.

Shift followed by CO_2 removal changes the conclusion because it changes the retained carbon inventory. The shift step preserves the deficit; removal reduces it by rejecting carbon. This distinction is useful when comparing conditioning sequences intended to retain plastic carbon. In a severely hydrogen-poor CO feed, shift can still enable some methanol formation by sacrificing other CO molecules as CO_2. The signed reaction network includes that possibility while retaining the same analytical upper bound.

E. Conditional recovery of methane carbon

Steam reforming introduces both hydrogen and carbon into the synthesis-gas pool. For each millimole of methane converted, 3 mmol H_2 and 1 mmol CO are formed. Converting that CO to methanol requires 2 mmol H_2, so the net reduction in the pre-existing deficit is only 1 mmol. Complete reforming of the measured 36.9 mmol CH_4 would thus lower the deficit from 74.0 to 37.1 mmol.

The carbon-oxide inventory would increase from 132.8 to 169.7 mmol, and the methanol ceiling without imported hydrogen would rise from 108.13 to 157.33 mmol. The increase of 49.2 mmol consists of 36.9 mmol newly admitted methane carbon and 12.3 mmol previously unsupported carbon-oxide carbon. Retention becomes 92.71% of the enlarged carbon-oxide pool; its denominator differs from that used for the untreated gas.

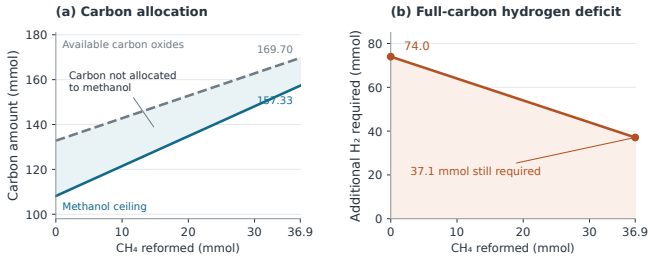

Figure 5: Conditional steam reforming of the measured methane. (a) Available carbon oxides and the methanol ceiling without added hydrogen; shading denotes carbon unsupported by the available hydrogen. (b) Additional hydrogen required for full conversion of the enlarged carbon-oxide pool. Full conversion of 36.9 mmol CH_4 leaves a 37.1 mmol hydrogen deficit. Conversion is prescribed, not experimentally measured

As Figure 5 shows, the methanol ceiling rises faster than the available carbon inventory. Their difference narrows by one-third of a millimole for every millimole of methane reformed, but remains 12.37 mmol at complete conversion of the measured methane. The plotted range ends at 36.9 mmol; extending it would assume an additional methane supply.

After complete methane reforming, full retention would still require 37.1 mmol external H_2. Alternatively, 12.37 mmol CO_2 removal would balance the retained gas without addition (Table 3). Counting the gross 110.7 mmol H_2 generated by reforming against the original 74.0 mmol deficit would miss the 73.8 mmol demand associated with the newly formed CO. The net balance is the relevant quantity for conditioning.

The result cannot be extended to unresolved hydrocarbons merely by counting their carbon atoms. Ideal steam reforming of C_nH_p changes the hydrogen deficit by $n - p/2$ moles per mole converted. Methane decreases it by one, ethene leaves it unchanged, and ethane decreases it by one while adding two carbon atoms. Steam conversion of hydrogen-free carbon increases the deficit. Identifying the C_{2+} species is therefore necessary before assigning them a conditioning benefit. Even for methane, the numerical result remains conditional on complete conversion and says nothing about the heat duty or catalyst required to achieve it.

Table 3: Effect of complete steam reforming of the measured 36.9 mmol CH_4. No external hydrogen is included in the methanol ceilings. Retention uses the available carbon-oxide inventory in each column, so the denominator changes after reforming

Quantity	Before conversion	After conversion
Carbon oxides (mmol)	132.80	169.70
Hydrogen deficit (mmol)	74.00	37.10
Methanol ceiling, no added H_2 (mmol)	108.13	157.33
Retention of available carbon oxides (%)	81.43	92.71
CO_2 removal for zero added H_2 (mmol)	24.67	12.37

F. Sensitivity to composition discrepancies

The hydrogen deficit stays positive at all corners of the prescribed $\pm 1\%$, $\pm 5\%$, and $\pm 10\%$ composition boxes. Its corresponding ranges are 68.67–79.33, 47.37–100.63, and 20.74–127.26 mmol. Thus, the sign of the conclusion is stable within these boxes, although the required adjustment varies substantially (Figure 6).

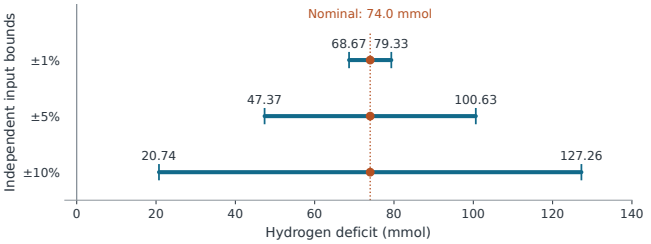

Figure 6: Exact deficit ranges under independent multiplicative bounds on H_2, CO, and CO_2. Endpoints are the extrema of Eq. (9); markers indicate the nominal 74.0 mmol deficit. Every interval remains above zero. These are deterministic sensitivity ranges, not confidence intervals

For the $\pm 5\%$ box, a fixed addition of 100.63 mmol H_2 ensures stoichiometric sufficiency without removal for every

ARCHIVES DES SCIENCES
A Multidisciplinary Journal

permitted composition. This is 35.99% above the nominal requirement. The increase reflects adverse deviations occurring together: hydrogen decreases while both carbon oxides increase. It is a worst-case design amount for the prescribed box, not a confidence limit on the experimental measurement.

Removal-only conditioning also has to remain feasible. In the $\pm 5\%$ box, a fixed removal of 33.54 mmol CO_2 is sufficient and remains below the minimum available CO_2 amount, 35.82 mmol. At the adverse $\pm 10\%$ corner, however, removing all CO_2 still leaves a 2.85 mmol hydrogen shortfall for the remaining CO (Table 4). No amount of selective CO_2 removal can correct that corner without another operation. The last column reports the largest such residual shortfall over each box, rather than the deficit after nominal conditioning.

A fixed setting must cover the most adverse composition before it is known. An adjustable setting can respond to measured composition but cannot remove more CO_2 than is present. The ten-percent result therefore limits even ideal adaptive removal. At five percent, a feasible fixed setting exists, but it rejects more carbon from the nominal gas than necessary.

The perturbation structure matters. Uniformly scaling all gas quantities changes absolute amounts while leaving S and carbon-retention fractions unchanged. Independent bounds permit the relative composition to change and are consequently more adverse. Neither construction is identified here with the actual instrument-error distribution. For the independent box, the deficit first reaches zero at a relative half-width of 13.89%, obtained directly from Eq. (9). This is an algebraic sign-change threshold, not an experimentally established detection limit.

Table 4: Sensitivity to independent bounds on the three gas quantities. Retention is evaluated without conditioning and uses each perturbed carbon-oxide inventory. The final column is the maximum hydrogen shortfall remaining after complete CO_2 removal, over the specified box

Half-width	Deficit interval (mmol)	Carbon retention interval (%)	Worst residual deficit after CO_2 removal (mmol)
1%	68.67–79.33	80.29–82.59	0
5%	47.37–100.63	75.94–87.48	0
10%	20.74–127.26	70.96–94.22	2.85

G. Numerical verification and electricity boundary

The analytical ceiling and linear-program objective agree over all 10,201 conditioning points, with a maximum absolute difference of 2.84×10^{-14} mmol. Eight additional boundary feeds cover empty gas, hydrogen-free CO, CO_2-only mixtures, exact stoichiometry, and excess hydrogen. The checks include both branches of the minimum in Eq. (4).

This agreement checks the implementation because the analytical and numerical calculations obtain the objective by different routes. Both nevertheless use the same input record and reaction set. They cannot detect every transcription error or establish whether a real catalyst approaches the bound. Experimental applicability must be assessed separately from numerical consistency.

The campaign H_2 and CO contain 92.49 kJ on the stated higher-heating-value basis. This subset represents 3.03% of the combined 2939.76 kJ electricity and 114.75 kJ polymer energy. Methane and unresolved products are excluded from the numerator, so the percentage is not a total energy-recovery efficiency. The polymer heating value in Supplementary Table 9 would give 114.775 kJ; the 0.025 kJ difference is consistent with rounding and does not justify changing the campaign entry.

Dividing recorded electricity by the unconditioned methanol ceiling gives 848.5 MJ kg^{-1}. At the full-carbon hydrogen-addition endpoint, the same electricity divided by the larger product ceiling gives 690.9 MJ kg^{-1}. Both are electricity-only lower bounds at the campaign scale. The latter omits production of the additional hydrogen, and neither includes synthesis compression, separation, or other downstream duties. The decrease therefore reflects a larger conditional denominator, not a demonstrated gain in total process efficiency.

Complete process assessments include those missing operations. Wind-to-methanol integration couples electrolysis and carbon capture with synthesis [33]; electrolysis life-cycle assessments include electricity and equipment inventories [34]; solar-powered hydrogen also retains life-cycle energy and emissions burdens [35]. The present ratios should consequently not be compared directly with whole-plant efficiency or greenhouse-gas indicators, nor should renewable electricity be removed from the physical energy balance.

H. Implications for process design

The nominal calculation identifies a choice between retaining carbon with imported hydrogen and reducing hydrogen demand through carbon rejection. Complete methane reforming improves both the product ceiling and hydrogen balance, but does not remove that choice. Selecting among these options requires information absent from the aggregate gas record: separation selectivity and duty, hydrogen supply, methanol conversion, catalyst lifetime, and product recovery.

Catalyst deactivation can change the preferred operating point over time [36]. The model contains no catalyst age, active surface area, pressure, water activity, or residence time and therefore cannot rank the untreated and CO_2-depleted feeds by productivity. Nor can the ten-batch hydrogen amount be converted directly into electrolyser capacity or buffer volume. Those require gas-delivery profiles, loading and cooling times, and a specified synthesis schedule.

Environmental claims require a wider boundary still. The mitigation potential of carbon utilization depends on energy and substitution assumptions [37]; comparisons of CO_2-derived one-carbon chemicals are sensitive to hydrogen and utilities [38]. Life-cycle guidance requires explicit functional units and boundaries [39], while compatibility with climate targets imposes conditions beyond incorporation of carbon into a product [40]. Methanol carbon retention alone establishes neither avoided emissions nor permanent storage.

The equations can be applied to another measured gas by replacing h, c, d, and the methane amount admitted to reforming. The present numerical endpoints, however, are specific to this campaign. Different polymers, contaminants, reforming conditions, and gas-cleaning losses require new inputs. The most useful next experiment would couple a fully speciated gas analysis with methanol-synthesis measurements before and after controlled conditioning, allowing the stoichiometric ceiling to be compared with actual carbon conversion and utility demand.

IV. Limitations and Reproducibility

The main empirical limitation is the use of one aggregate gas record. Replicate covariance, batch-to-batch composition, and delivery rates are unavailable. The prescribed perturbations measure sensitivity to chosen input bounds; they do not estimate analytical uncertainty or variability across waste-plastic feeds. The ambiguous C_{2+} group also prevents a complete molecular and feed-carbon balance.

The stoichiometric model assumes unrestricted water availability, selective CO_2 removal, and the stated reaction set. It excludes equilibrium restrictions, kinetic limitations, side products, catalyst poisoning, and losses during product recovery. Complete methane reforming is a conditional case. Trace contaminants and gas-cleaning requirements remain uncharacterized, so a balanced major-species composition does not certify a synthesis-ready feed. These omissions limit the use of the results for reactor, separator, or compressor design.

V. Conclusion

The ten-batch polyethylene-derived gas is hydrogen deficient for complete conversion of its carbon oxides to methanol, despite an H_2/CO ratio of 2.411. Its stoichiometric number is 1.443 and its hydrogen deficit is 74.0 mmol. Adding that amount of hydrogen permits a 132.8 mmol methanol ceiling. Selectively removing 24.67 mmol CO_2 instead balances the retained gas without increasing the untreated ceiling of 108.13 mmol, or 81.43% of the initial carbon-oxide carbon.

Water–gas shift cannot close the deficit because the hydrogen generated is matched by the additional demand of the CO_2 formed. Complete reforming of the measured methane would raise the methanol ceiling to 157.33 mmol while leaving a 37.1 mmol deficit for the enlarged carbon pool. The shortage also persists across the prescribed $\pm 5\%$ composition box, for which guaranteed full-carbon sufficiency without removal requires 100.63 mmol added hydrogen.

Gas conditioning should be assessed against both hydrogen demand and retained carbon. These material limits guide experimental comparisons; practical operation still requires measured synthesis performance and complete accounting of hydrogen, gas-cleaning, separation, and product-recovery duties.

Author Contributions

Both authors contributed equally to the conception, development, and preparation of the manuscript. Both authors have read and approved the final version of the manuscript for publication.

Data Availability

All data required to support the findings of this study are included within the manuscript.

Conflicts of Interest

The authors declare that there are no conflicts of interest related to this work.

Funding

This research received no external funding.

Use of Computational and AI-Assisted Tools

Artificial intelligence and computational tools were used to assist with code generation, consistency checking, and technical refinement during the preparation of the manuscript. All AI-assisted and computationally generated content was carefully reviewed and verified by the authors, who take full responsibility for the accuracy, integrity, and final content of the manuscript.

References

[1] Geyer, R., Jambeck, J. R., & Law, K. L. (2017). Production, use, and fate of all plastics ever made. *Science Advances*, *3*(7), Article e1700782.

[2] Zheng, J., & Suh, S. (2019). Strategies to reduce the global carbon footprint of plastics. *Nature Climate Change*, *9*(5), 374–378.

[3] Meys, R., Kätelhön, A., Bachmann, M., Winter, B., Zibunas, C., Suh, S., & Bardow, A. (2021). Achieving net-zero greenhouse gas emission plastics by a circular carbon economy. *Science*, *374*(6563), 71–76.

[4] Bachmann, M., Zibunas, C., Hartmann, J., Tulus, V., Suh, S., Guillén-Gosálbez, G., & Bardow, A. (2023). Towards circular plastics within planetary boundaries. *Nature Sustainability*, *6*(5), 599–610.

[5] Uekert, T., Singh, A., DesVeaux, J. S., Ghosh, T., Bhatt, A., Yadav, G., Afzal, S., Walzberg, J., Knauer, K. M., Nicholson, S. R., Beckham, G. T., & Carpenter, A. C. (2023). Technical, economic, and environmental comparison of closed-loop recycling technologies for common plastics. *ACS Sustainable Chemistry & Engineering*, *11*(3), 965–978.

[6] Nixon, K. D., Schyns, Z. O. G., Luo, Y., Ierapetritou, M. G., Vlachos, D. G., Korley, L. T. J., & Epps, T. H., III (2024). Analyses of circular solutions for advanced plastics waste recycling. *Nature Chemical Engineering*, *1*(10), 615–626.

[7] Yao, D., Yang, H., Chen, H., & Williams, P. T. (2018). Investigation of nickel-impregnated zeolite catalysts for hydrogen/syngas production from the catalytic reforming of waste polyethylene. *Applied Catalysis B: Environmental*, *227*, 477–487.

[8] Acomb, J. C., Wu, C., & Williams, P. T. (2014). Control of steam input to the pyrolysis-gasification of waste plastics for improved production of hydrogen or carbon nanotubes. *Applied Catalysis B: Environmental*, *147*, 571–584.

[9] Zhang, Y., Huang, J., & Williams, P. T. (2017). Fe–Ni–MCM-41 catalysts for hydrogen-rich syngas production from waste plastics by pyrolysis–catalytic steam reforming. *Energy & Fuels*, *31*(8), 8497–8504.

[10] Li, Y., Nahil, M. A., & Williams, P. T. (2023). Hydrogen/syngas production from different types of waste plastics using a sacrificial tire char catalyst via pyrolysis–catalytic steam reforming. *Energy & Fuels*, *37*(9), 6661–6673.

[11] Ma, Q., Gao, Y., Sun, B., Du, J., Zhang, H., & Ma, D. (2024). Grave-to-cradle dry reforming of plastics via Joule heating. *Nature Communications*, *15*, Article 8243.

[12] Wismann, S. T., Engbæk, J. S., Vendelbo, S. B., Bendixen, F. B., Eriksen, W. L., Aasberg-Petersen, K., Frandsen, C., Chorkendorff, I., & Mortensen, P. M. (2019). Electrified methane reforming: A compact approach to greener industrial hydrogen production. *Science*, *364*(6442), 756–759.

[13] Mion, A., Galli, F., Mocellin, P., Guffanti, S., & Pauletto, G. (2022). Electrified methane reforming decarbonises methanol synthesis. *Journal of CO_2 Utilization*, *58*, Article 101911.

[14] From, T. N., Partoon, B., Rautenbach, M., Østberg, M., Bentien, A., Aasberg-Petersen, K., & Mortensen, P. M. (2024). Electrified steam methane reforming of biogas for sustainable syngas manufacturing and next-generation of plant design: A pilot plant study. *Chemical Engineering Journal*, *479*, Article 147205.

[15] Wismann, S. T., Engbæk, J. S., Vendelbo, S. B., Eriksen, W. L., Frandsen, C., Mortensen, P. M., & Chorkendorff, I. (2021). Electrified methane reforming: Elucidating transient phenomena. *Chemical Engineering Journal*, *425*, Article 131509.

[16] Ribeiro, A. M., Santos, J. C., Rodrigues, A. E., & Rifflart, S. (2012). Syngas stoichiometric adjustment for methanol production and co-capture of carbon dioxide by pressure swing adsorption. *Separation Science and Technology*, *47*(6), 850–866.

[17] Laudenschleger, D., Ruland, H., & Muhler, M. (2020). Identifying the nature of the active sites in methanol synthesis over $Cu/ZnO/Al_2O_3$ catalysts. *Nature Communications*, *11*, Article 3898.

[18] Frei, M. S., Capdevila-Cortada, M., García-Muelas, R., Mondelli, C., López, N., Stewart, J. A., Curulla-Ferré, D., & Pérez-Ramírez, J. (2018). Mechanism and microkinetics of methanol synthesis via CO_2 hydrogenation on indium oxide. *Journal of Catalysis*, *361*, 313–321.

[19] Behrens, M., Studt, F., Kasatkin, I., Kühl, S., Hävecker, M., Abild-Pedersen, F., Zander, S., Girgsdies, F., Kurr, P., Kniep, B.-L., Tovar, M., Fischer, R. W., Nørskov, J. K., & Schlögl, R. (2012). The active site of methanol synthesis over $Cu/ZnO/Al_2O_3$ industrial catalysts. *Science*, *336*(6083), 893–897.

[20] Kiss, A. A., Pragt, J. J., Vos, H. J., de Groot, M. T., & Bargeman, G. (2016). Novel efficient process for methanol synthesis by CO_2 hydrogenation. *Chemical Engineering Journal*, *284*, 260–269.

[21] Pérez-Fortes, M., Schöneberger, J. C., Boulamanti, A., & Tzimas, E. (2016). Methanol synthesis using captured CO_2 as raw material: Techno-economic and environmental assessment. *Applied Energy*, *161*, 718–732.

[22] Harris, K., Grim, R. G., Huang, Z., & Tao, L. (2021). A comparative techno-economic analysis of renewable methanol synthesis from biomass and CO_2: Opportunities and barriers to commercialization. *Applied Energy*, *303*, Article 117637.

[23] Mucci, S., Mitsos, A., & Bongartz, D. (2023). Cost-optimal power-to-methanol: Flexible operation or intermediate storage? *Journal of Energy Storage*, *72*, Article 108614.

[24] Zheng, Y., You, S., Li, X., Bindner, H. W., & Münster, M. (2022). Data-driven robust optimization for optimal scheduling of power to methanol. *Energy Conversion and Management*, *256*, Article 115338.

[25] Ma, Q., Gao, Y., Cai, C., Wang, T., & Ma, D. (2025). Syngas from waste plastics and water using Joule heating. *Nature Communications*, *16*, Article 6015.

[26] Ambrosetti, M., Beretta, A., Groppi, G., & Tronconi, E. (2021). A numerical investigation of electrically-heated methane steam reforming over structured catalysts. *Frontiers in Chemical Engineering*, *3*, Article 747636.

[27] Bertsimas, D., Gupta, V., & Kallus, N. (2018). Data-driven robust optimization. *Mathematical Programming*, *167*(2), 235–292.

[28] Harris, C. R., Millman, K. J., van der Walt, S. J., Gommers, R., Virtanen, P., Cournapeau, D., Wieser, E., Taylor, J., Berg, S., Smith, N. J., Kern, R., Picus, M., Hoyer, S., van Kerkwijk, M. H., Brett, M., Haldane, A., Fernández Del Río, J., Wiebe, M., Peterson, P., . . . Oliphant, T. E. (2020). Array programming with NumPy. *Nature*, *585*(7825), 357–362.

[29] Virtanen, P., Gommers, R., Oliphant, T. E., Haberland, M., Reddy, T., Cournapeau, D., Burovski, E., Peterson, P., Weckesser, W., Bright, J., van der Walt, S. J., Brett, M., Wilson, J., Millman, K. J., Mayorov, N., Nelson, A. R. J., Jones, E., Kern, R., Larson, E., . . . SciPy 1.0 Contributors (2020). SciPy 1.0: Fundamental algorithms for scientific computing in Python. *Nature Methods*, *17*(3), 261–272.

[30] Huangfu, Q., & Hall, J. A. J. (2018). Parallelizing the dual revised simplex method. *Mathematical Programming Computation*, *10*(1), 119–142.

[31] Hunter, J. D. (2007). Matplotlib: A 2D graphics environment. *Computing in Science & Engineering*, *9*(3), 90–95.

[32] Kuld, S., Thorhauge, M., Falsig, H., Elkjær, C. F., Helveg, S., Chorkendorff, I., & Sehested, J. (2016). Quantifying the promotion of Cu catalysts by ZnO for methanol synthesis. *Science*, *352*(6288), 969–974.

[33] Bos, M. J., Kersten, S. R. A., & Brilman, D. W. F. (2020). Wind power to methanol: Renewable methanol production using electricity, electrolysis of water and CO_2 air capture. *Applied Energy*, *264*, Article 114672.

[34] Bareiß, K., de la Rua, C., Möckl, M., & Hamacher, T. (2019). Life cycle assessment of hydrogen from proton exchange membrane water electrolysis in future energy systems. *Applied Energy*, *237*, 862–872.

[35] Palmer, G., Roberts, A., Hoadley, A., Dargaville, R., & Honnery, D. (2021). Life-cycle greenhouse gas emissions and net energy assessment of large-scale hydrogen production via electrolysis and solar PV. *Energy & Environmental Science*, *14*(10), 5113–5131.

[36] Fichtl, M. B., Schlereth, D., Jacobsen, N., Kasatkin, I., Schumann, J., Behrens, M., Schlögl, R., & Hinrichsen, O. (2015). Kinetics of deactivation on $Cu/ZnO/Al_2O_3$ methanol synthesis catalysts. *Applied Catalysis A: General*, *502*, 262–270.

[37] Kätelhön, A., Meys, R., Deutz, S., Suh, S., & Bardow, A. (2019). Climate change mitigation potential of carbon capture and utilization in the chemical industry. *Proceedings of the National Academy of Sciences*, *116*(23), 11187–11194.

[38] Sternberg, A., Jens, C. M., & Bardow, A. (2017). Life cycle assessment of CO_2-based C1-chemicals. *Green Chemistry*, *19*(9), 2244–2259.

[39] Müller, L. J., Kätelhön, A., Bachmann, M., Zimmermann, A., Sternberg, A., & Bardow, A. (2020). A guideline for life cycle assessment of carbon capture and utilization. *Frontiers in Energy Research*, *8*, Article 15.

[40] de Kleijne, K., Hanssen, S. V., van Dinteren, L., Huijbregts, M. A. J., van Zelm, R., & de Coninck, H. (2022). Limits to Paris compatibility of CO_2 capture and utilization. *One Earth*, *5*(2), 168–185.